PREDICTIONS OF GAS-PARTICLE PARTITIONING COEFFICIENTS (K_P) OF POLYCYCLIC AROMATIC HYDROCARBONS AT VARIOUS OCCUPATIONAL ENVIRONMENTS OF SONGKHLA PROVINCE, THAILAND

S Pongpiachan[1,2], K Thamanu[3], KF Ho[4], SC Lee[4] and P Sompongchaiyakul[5,6]

[1]Biogeochemical and Environmental Change Research Unit, Faculty of Environmental Management, [2]National Center of Excellence for Environmental and Hazardous Waste Management-PSU Satellite Center, Prince of Songkla University, Hat Yai, Songkhla Thailand; [3]Synchrotron Light Research Institute, Ministry of Science and Technology, Nakhon Ratchasima, Thailand; [4]Research Center for Environmental Technology and Management, Department of Civil and Structural Engineering, Hong Kong Polytechnic University, Hong Kong, China; [5]Department of Marine Science, Faculty of Science, Chulalongkorn University, Bangkok; [6]National Center of Excellence for Environmental and Hazardous Waste Management, Bangkok, Thailand

Abstract. Ambient air samples were collected over periods of 24 hours and 3 hours using a Graseby-Anderson high volume air sampler with PM_{10} TE-6001 at 15 sampling sites, including an urban residential zone, rural area, industrial factories, waste incinerator, traffic areas and agricultural burning areas in Songkhla Province, Thailand. An analysis of organic carbon and elemental carbon was conducted to estimate the gas-particle partitioning of PAHs using a model proposed by Dachs-Eisenreich. The estimated LogK_P of PAHs emphasized the risk for lung cancer among outdoor workers in waste incinerators, traffic intersections and bus terminals, suggesting the role of the carbonaceous fraction over the gas-particle partitioning of PAHs. Analysis of $f_{SC}K_{SA}\delta_{OCT}/f_{OM}K_{OA}$ ratios revealed a significant role of *ad*sorption and *ab*sorption in unusually high elemental carbon fractions (*ie* low OC/EC ratio) in fine particles collected at waste incinerators and the abnormally high organic carbon fractions (*ie* high OC/EC ratio) observed in those fine particles of an urban residential zone, respectively. The dual mode of *ab*/*ad*sorption tended to dominate the gas-particle partitioning of LMW PAHs collected at the traffic intersections and bus terminal.

INTRODUCTION

Carbonaceous aerosol is a main contributor to environmental and health problems (Na and Cocker, 2005; Hu *et al*, 2007). Generally, two types of carbonaceous aerosol exist in the atmospheric environment, namely organic carbon (OC) and elemental carbon (EC). Many studies have shown strong associations between the amount of OC/EC and gas particle partitioning of polycyclic aromatic hydrocarbons (PAHs) (Dachs and Eisenreich, 2000; Fernandez *et al*, 2002; Vardar *et al*, 2004; Tasdemir and Esen, 2007). PAHs are ubiquitous pollutants in the atmospheric environment, generally containing two to eight benzene rings and can be pro-

Correspondence: S Pongpiachan, Biogeochemical and Environmental Change Research Unit, Faculty of Environmental Management, Prince of Songkla University, Hat Yai, Songkhla 90112, Thailand.
Tel: 66 (0) 7428 6838; Fax: 66 (0) 7442 9758
E-mail: pongpiajun@gmail.com

duced by natural (volcanic eruptions, forest fires) and anthropogenic (traffic emissions, industrial activities, aluminium production, domestic heating and tobacco smoking) processes (Harvey, 1991; Menzie *et al*, 1992; Mastral and Callén, 2000; Sanderson and Farant, 2000; Korenaga *et al*, 2001; Ohura *et al*, 2004; Repace, 2004).

PAHs have received attention because some of these compounds are considered to be toxic, carcinogenic and/or mutagenic (IARC, 1987, 1997; WHO, 2000). Gas-particle partitioning benefits both the prediction of PAHs in different environmental compartments and the assessment of respiratory health effects, since the risk of inhaling PAHs depends in part on whether they exist in vapor or particulate phase (Pankow, 2001). Fernandez *et al* (2002) proposed the concept of the gas-particle partitioning coefficient (K_p) as a main mechanism behind the global distribution of PAHs via long range transport. Over the past few decades a comprehensive physicochemical investigation of gas-particle partitioning has been conducted in order to predict the K_p of PAHs. By assuming the gas-particle partitioning of PAHs was governed by both *ab*sorption and *ad*sorption processes, the K_p values can be estimated using the octanol/air partition coefficient (K_{OA}) and soot/air partition coefficient (K_{SA}) as found in Equation 1:

$$K_P = \frac{f_{OM}}{\rho_{OCT} 10^{12}} K_{OA} + f_{EC} \frac{a_{EC}}{10^{12} a_{AC}} K_{SA}$$

Equation 1

where ρ_{oct} (820 kg m^{-3} at 20ºC), f_{OM},f_{EC}, a_{AC}, a_{EC} are the density of the octanol, the fraction of organic matter, the fraction of elemental carbon, the surface area of the activated carbon and the surface area of elemental carbon, respectively. When the partitioning is occupied by both *ad*sorptive and *ab*sorptive processes, K_p can be predicted using the Dachs-Eisenreich model (Equation1).

Although many researchers highlight the role of *ad*sorption onto black carbon (BC) surfaces and *ab*sorption into the organic layer as two major sorption mechanisms, only a few middle MW PAH compounds were investigated. Little is known about the gas-particle partitioning processes of low and high MW PAH compounds as it can be explained by the lack of experimental K_{SA} values (Ribes *et al*, 2003). Both K_{SA} and K_{OA} can be significantly influenced by temperature, which emphasizes the importance of minimizing temperature fluctuations. Recently, Odabasi *et al* (2006) determined octanol-air partition coefficients (K_{OA}) and super-cooled liquid vapor pressure (P_L) for 13 PAHs, namely: acenaphthylene (Ac), acenaphthene (Ace), fluorene (Fl), phenanthrene (Ph), anthracene (An), fluoranthene (Fluo), pyrene (Pyr), benzo[*a*]anthracene (B[*a*]A), chrysene (Chry), benzo[*a*]pyrene (B[*a*]P), indeno[*1,2,3-cd*]pyrene (Ind), dibenz[*a,h*]anthracene (D[*a,h*]A) and benzo[*g,h,i*]perylene (B[*g,h,i*]P) as a function of temperature using the gas chromatographic retention time technique. The temperature dependence of K_{OA} can be obtained by:

$$\log K_{OA} = A + \frac{B}{T}$$

Equation 2

where *A* and *B* were calculated by Harner and Bidleman (1998 a, b). In this study, K_{SA} values for PAHs were estimated as a function of super-cooled liquid vapor pressure (P_L) and elemental carbon specific surface area (a_{EC}, m^2 g^{-1}) as can be seen in Equation 3 as described by Odabasi *et al* (2006):

$$\log K_{SA} = -0.85 \log P_L + 8.94 - \log(\frac{998}{a_{EC}})$$

Equation 3

where the a_{EC} value of 62.7 m^2 g^{-1} was reported by Jonker and Koelmans (2002) and

can be obtained using the intercept b_L, slope m_L and temperature T as seen in Equation 4 (Odabasi *et al* (2006):

$$\log P_L(Pa) = m_L(T,K)^{-1} + b_L$$

Equation 4

In the present work, we report the gas-particle partitioning coefficients (K_P) of PAHs estimated using the Dachs-Eisenreich model with the measured OC/EC values of the fine particle-PM_{10} (aerodynamic diameter <10 μm) from 15 sources in Songkhla Province, Thailand.

Rapid industrialization, urbanization, economic and population growth, and increasing use of motor vehicles all contribute to air pollution in urban areas. Songkhla's air quality has steadily deteriorated over the past ten years. This is commonly seen in cities with economic growth. This study estimated K_P values of PAHs in PM_{10} from different occupational atmospheric environments in Songkhla Province, Thailand. The results obtained in this study allow assessment of various emission sources on air quality and assist the policy maker in making policy decisions and control strategies to allow for occupational inhalation disease reduction. Given the increasing number of vehicles, industrial factories, para-rubber tree manufacturing factories and trans-boundary biomass burnings from neighbor countries, more studies are required to understand the carcinogenic emission source strengths and released chemical compositions from various emission sources. In light of the various sources of pollution in the atmosphere, the challenge for local authorities is to find the most appropriate way of reducing carcinogenic pollutants. Since PAHs are continuously released into the atmosphere, raising concerns over the safety of urban residents and those who are living or working adjacent to the emission sources, it is crucial to investigate occupational exposure to PM_{10}, carbonaceous aerosols and the influence of OC/EC over the gas-particle partitioning of PAHs released in different working environments.

MATERIALS AND METHODS

Sampling sites

The population of the Songkhla Province is about 1.32 million people occupying 7,394 km^2. Songkhla is located 950 km south of Bangkok, situated on the eastern side of the Malayan Peninsula, bordered by Nakhon Si Thammarat and Phatthalung in the north; Yala, Pattani, Kedah (Sai Buri) and Perlis, Malaysia in the south; the Gulf of Thailand to the east; Satun and Phatthalung Provinces to the west (Fig 1). Hat Yai, a district of Songkhla, is better known than the provincial capital itself, as an economic and tourist zone of Songkhla and has numerous industrial factories and stores located in this area. Sampling site descriptions are given in Table 1.

Sample collection

Ambient air samples were collected over periods of 24 hours and 3 hours using a Graseby-Anderson high volume air sampler with PM_{10} TE-6001, operating at a flow rate of 1.4 $m^3\ min^{-1}$. A total of 51 air samples were acquired using high volume yielding sample volumes of approximately 2,016 m^3 and 252 m^3 for each 24 hours and 3 hours sample, respectively. Twenty-four hour sampling was conducted for three consecutive days at PSU, TI, CI, CPF, SL, RMF, BT, WI, BF, PR and KHH stations. The air samples collected at RSB, BB and PTB stations represent the periods of air quality that were the most contaminated. The 3-hour samples were collected three times per day in order to avoid an overload of air particulate matter at the three stations.

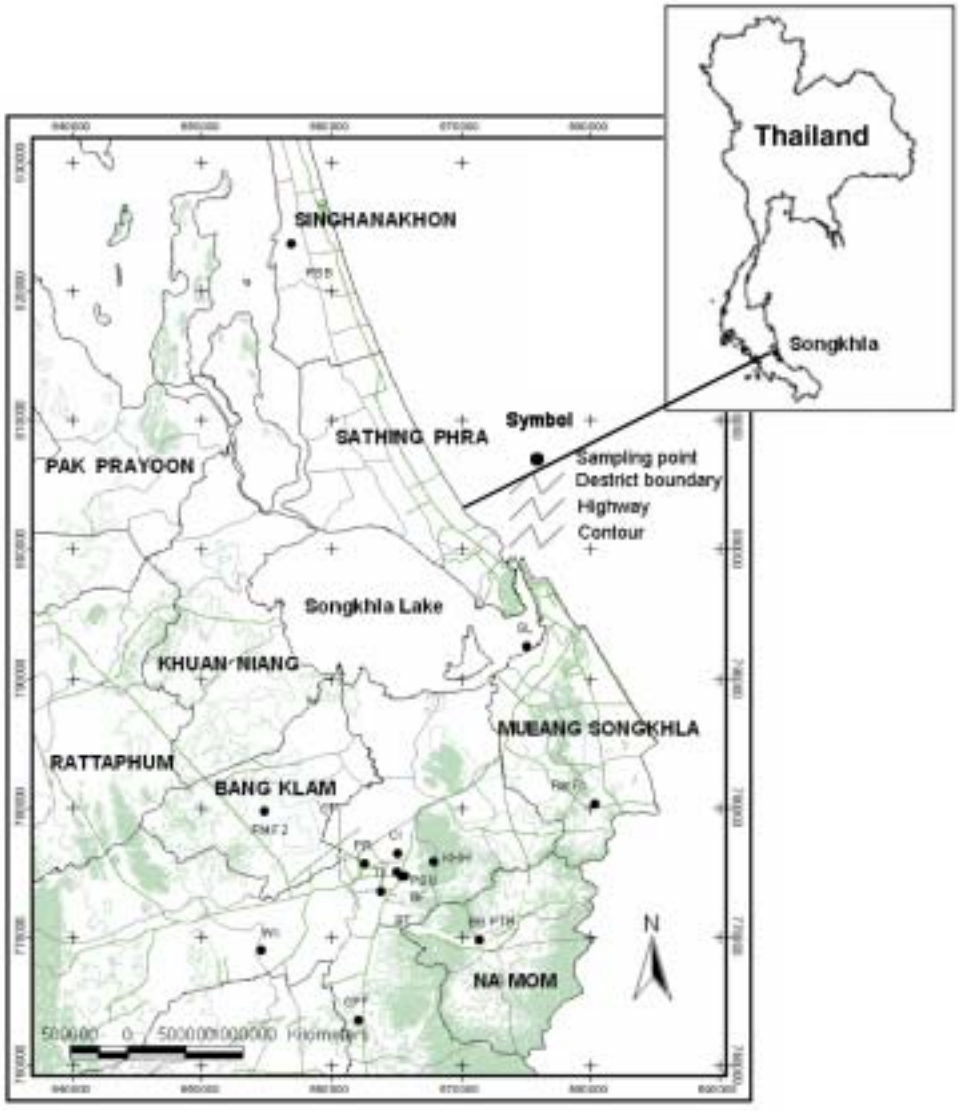

Fig 1–Map of sampling sites.

PM_{10} was collected on 47 mm Whatman quartz microfiber filters (QM/A). The filters were pre-heated at 800°C for 12hours prior to sampling. The exposed filters were stored in a refrigerator at about 4°C until chemical analysis to prevent evaporation of volatile compounds. Field blank filters were also collected to assess any potential contamination of carbonaceous components on the filter before/during/after sampling. The positive artifact due to both *ab*sorption and *ad*sorption of gaseous organic compounds onto the filters was subtracted. However, negative artifacts related to volatilization of

particulate organic compounds on the filter were not quantified in this study. All field sampling and filter weighing were performed in compliance with the US EPA's guidelines for Standard Operating Procedures for sampling and handling of $PM_{2.5}$ filters. In addition, all filters were weighed with a Mettler Toledo AB204-S analytical balance before sending to the Department of Civil and Structural Engineering, Research Center for Environmental Technology and Management, Hong Kong Polytechnic University for carbonaceous aerosol analysis.

Carbonaceous aerosol analysis

Carbon analysis was carried out at the laboratory of the Department of Civil and Structural Engineering, Research Center for Environmental Technology and Management, Hong Kong Polytechnic University, China. The samples were analyzed for OC and EC using a DRI Model 2001 Thermal/Optical Carbon Analyzer with the IMPROVE thermal/optical reflectance (TOR) protocol. The protocol calls for heating a 0.526 cm^2 punch aliquot of a sample quartz filter stepwise to temperatures of 120°C (OC1), 250°C (OC2), 450°C (OC3), and 550°C (OC4) in a non-oxidizing helium atmosphere, and 550°C (EC1), 700°C (EC2), and 800°C (EC3) in an oxidizing atmosphere of 2% oxygen in a balance of helium. When oxygen was added, the original and pyrolized black carbon burned and the reflectance increased. The amount of carbon measured after oxygen was added until the reflectance achieved its original value was reported as the optically-detected pyrolized carbon (OP).

Model description

Two different mechanisms have been employed to describe the gas-particle partition of PAHs, namely physical *ad*sorption onto the aerosol surface and chemical *ab*sorption into the aerosol organic layer (Dachs and Eisenreich, 2000). Both mechanisms lead to a linear relationship between log K_p and log P_L^o (Junge-Pankow Sorption Model), where P_L^o is the compound's subcooled liquid vapor pressure and K_p is the gas particle partitioning coefficient (Pankow, 1994a, b). When the partitioning is dominated by *ad*sorption, K_p can be expressed by:

$$K_p = \frac{C_p}{C_g TSP} = \frac{N_s a_{TSP} T e^{(Q_l - Q_v)/RT}}{16 P_L^\circ}$$

Equation 5

where C_p and C_g are the particle and gas phase concentrations (in ng m^{-3}), respectively. N_s is the number of *ad*sorption sites (per cm^{-2}), a_{TSP} is the surface area of TSP (in $m^2\ g^{-1}$), T is the temperature (in K), R is the universal gas constant (8.3 x 10^{-3} kJ K^{-1} mol^{-1}), and Q_l and Q_v are the enthalpies of *de*sorption and volatilization (in kJ mol^{-1}), respectively, and P_L^o is the compound's subcooled liquid vapor pressure (Torr). Experimentally, P_L^o can be determined by using different methods. Many of the parameters (*eg*, N_s, a_{TSP}, Q_1 and Q_v) are unknown for atmospheric aerosols. Thus, it is difficult to achieve a precise K_p prediction based on Equation 5. The gas-particle partitioning of PAHs (K_p) can be determined using Equation 6 as a function of P_L^o involving both *ad*sorptive and *ab*sorptive partitioning mechanisms.

$$\log K_p = m_r \log P_L^\circ + b_r$$

Equation 6

In Equation 6 m_r and b_r are empirical constants, regardless of the partitioning mechanism. At equilibrium, the slope for either *ad*sorption or *ab*sorption should be close to -1 given the assumptions that, for *ad*sorption, the differences between the enthalpies of *de*sorption and volatilization and the number of available *ad*sorption sites

must remain constant over a compound class as must the activity coefficients for *ab*sorption (Vardar *et al*, 2004). However, the slopes and intercepts yielded from several field measurements worldwide are diverse, and while some are near the theoretical values, significant deviations have been reported (Simcik *et al*, 1998; Sitaras *et al*, 2004; Vardar *et al*, 2004). Several processes have been used to explain these deviations such as disequilibrium and/or sampling artifacts, which might lead to steeper or shallower gradients than -1.

During the past few years, an intense research effort has been made to develop the modeling framework for the sorption processes in order to predict the gas/particle partitioning of PAHs. Fenizio *et al* (1997) proposed a method to predict K_p values for a wide range PAHs using only the octanol/air partition coefficient (K_{OA}) assuming that *ab*sorption is the main sorption process:

$$K_P = \frac{f_{OM} MW_{OCT} \gamma_{OCT}}{\rho_{OCT} MW_{OM} \gamma_{OM} 10^{12}} K_{OA}$$

Equation 7

where ρ_{oct} (0.824 kg L^{-1} at 20ºC) is the density of octanol and γ are the activity coefficients of the PAHs in organic matter (OM) and octanol (oct), respectively. Assuming that *ab*sorption is the dominant sorption process and $MW_{oct}/MW_{OM} = \gamma_{oct}/\gamma_{OM} = 1$, Equation 7 can then be simplified to:

$$Log\, K_P = Log\, K_{OA} + Log\, f_{OM} - 11.91$$

Equation 8

Equation 8 was developed from the Pankow model where both K_p and P_L^o were used as descriptors for *ab*sorptive partitioning. The *ab*sorptive model may also be expressed as:

$$K_P = \frac{f_{OM}\, 760 RT}{MW_{OM} \gamma P_L^\circ}$$

Equation 9

where f_{OM} is the fraction of OM and γ are the activity coefficients of PAHs in OM. The chief advantage of using K_{OA} is that K_{OA} can be measured directly, whereas P_L^o and other parameters in the prediction models are often unknown or experimentally inaccessible. The K_{OA} *ab*sorption model (Equation 8) can predict gas-particle partitioning of PAHs from knowledge of only K_{OA} and the organic fraction of the particle, if the partitioning is dominated by *ab*sorption into organic matter present in the particle. In contrast to OM partitioning, several researchers have studied the prominent role of elemental carbon (EC) *ad*sorption in the atmosphere. Dachs and Eisenreich (2000) reported the evidence for *ad*sorption to EC is dominating the gas-particle partitioning in the New Jersey atmosphere. Assuming that EC is a surrogate for the soot phase, the overall gas-particle partitioning coefficient that accounts for both the organic matter and the soot phases is given by Equation 1. The major advantage of this model is a combination of two gas-particle partitioning mechanisms into a single model, thus one can assume better predictions than using the individual *ab*sorption or *ad*sorption model. However, several concerns remain over uncertainties of the octanol/air partition coefficient (K_{OA}) and the soot/air partition coefficient (K_{SA}) coupled with the method used for OC/EC analysis. Therefore, data interpretation should be made with great caution due to the parameter and analytical uncertainties described above.

RESULTS

Table 1 reveals the ambient temperature and air pressure readings at the 15 sites were

similar during the study period regardless of the different emission source characteristics. The relative standard deviation (RSD) of the ambient temperatures and air pressures measured were 6.4 and 0.07%, respectively. The lack of spatial variation in ambient temperature and the high air pressure at the sampling sites could be due to the equatorial climate where there is no winter and mostly good weather. The RSD of the relative humidity had a peak value of 11.8%. Since air masses formed over oceans generally contain more moisture than continental ones, it seems reasonable to ascribe the high RSD for relative humidity to this.

Different patterns were observed for organic carbon (OC) and elemental carbon (EC) concentrations in PM_{10} (Table 2). Since the RSD of OC was 149%, there was a spatial variation for OC, with the highest concentration at the RSB (64.992 ± 51.974 μg m^{-3}) and the lowest level at the SL2 (0.757 ± 0.397 μg m^{-3}) during the study period. The high levels of OC aerosol observed in the RSB (64.992 ± 51.974 μg m^{-3}), PTB (38.578 ± 35.154 μg m^{-3}) and RMF1 (10.852 ± 17.158 μg m^{-3}) reflect directly on the primary emission sources of biomass burning. The average concentration of OC observed at SL2 (0.757 ± 0.397 μg m^{-3}) was lower than others, due to its distance from the urban district of Hat Yai and "the dilution effect" triggered by clean maritime air from the Gulf of Thailand (Fig 1). There was a significant temporal difference in EC levels, with the maximum value at WI (19.023 ± 31.442 μg m^{-3}) and a minimum value at SL2 (0.221 ± 0.401 μg m^{-3}). Since EC is mainly emitted from combustion sources and is not generated by secondary chemical reactions in the atmosphere, it is not surprising the highest and lowest levels of EC were observed at WI and SL2, respectively. It is worth mentioning the incinerator at WI was specially designed for burning infected waste, such as surgical instruments, wound cotton, bed sheets and biological materials collected from hospitals located in Songkhla Province. Hence, the incineration temperature was kept between 700 and 1,200°C to ensure adequate destruction of pathogenic heat-resistant organisms. With this process the majority of OC will be destroyed, leaving only EC in the exhausted aerosols. It is interesting to see the EC concentration and fraction (f_{EC}) of WI were higher than the traffic emission sources (*ie*, PR, TI and BT) by 3.0 to 4.5 times, raising concerns of urban air pollution caused by uncontrolled burning of municipal waste.

The total carbonaceous aerosol (TCA) was estimated by the sum of organic matter and elemental carbon. The organic matter can be calculated by multiplying the amount of OC by 1.6 (Turpin and Lim, 2001). PM_{10} at PSU1 and PSU2 consisted of 18.7% and 17.6% of the TCA, respectively. The percentage contributions of TCA observed at the traffic sites were: 31.6% (TI), 33.0% (BT) and 38.4% (PR). Since all the sampling stations were close to the Gulf of Thailand within a distance of 22 km, it seems reasonable to conclude the atmospheric dilution caused by clean maritime air contributed to the low percentages of TCA in the urban residential zone of Hat Yai. It is a crucial to note that Hat Yai has a lower population (only 157,000) compared to Hong Kong (7 million), Guangzhou (8.5 million), Shenzhen (8.6 million) and Zhuhai (1.5 million). This can explain the relatively low TCA observed in Hat Yai. Climate zone classification explains the relatively lower TCA of Hat Yai atmosphere. Unlike conventional temperate zone cities, Hat Yai has a tropical climate with a higher temperature and greater solar radiation. Under this condition, ultraviolet photolysis is greater, thus decomposing the TCA into a lower level.

Table 1
Statistical descriptions of meteorological parameters and sampling positions.

Site	Source type	Sampling period	Latitude	Longitude	Average T[1] [ºC]	Average RH[2] [%]	Average AP[3] [mbar]
PSU1	Urban residential zone	28/06/07-30/06/07	7º 00' 21.28'' N	100º 29' 53.27'' E	30 ± 3	66 ± 20	1,007.8 ± 1.5
PSU2	Urban residential zone	24/10/07-26/10/07	7º 00' 21.28'' N	100º 29' 53.27'' E	28 ± 2	73 ± 11	1,009.0 ± 1.6
TI	Traffic	05/07/07-07/07/07	7º 00' 30.81'' N	100º 29' 39.21'' E	27 ± 3	79 ± 12	1,008.1 ± 1.0
CI	Timber	19/07/07-21/07/07	7º 01' 17.55'' N	100º 29' 41.44'' E	32 ± 3	61 ± 13	1,007.4 ± 0.6
CPF	Crude oil	24/07/07-26/07/07	6º 54' 16.38'' N	100º 28' 05.15'' E	32 ± 1	65 ± 6	1,007.8 ± 0.6
SL1	Rural background	27/07/07-29/07/07	7º 10' 02.92'' N	100º 35' 11.36'' E	29 ± 2	68 ± 10	1,006.8 ± 0.6
SL2	Rural background	20/10/07-22/10/07	7º 10' 02.92'' N	100º 35' 11.36'' E	31 ± 0	59 ± 3	1,007.1 ± 1.0
RMF1	Timber	30/07/07-01/08/07	7º 03' 19.97'' N	100º 37' 58.90'' E	30 ± 1	69 ± 9	1,008.1 ± 1.0
RMF2	Timber	02/08/07-04/08/07	7º 03' 06.28'' N	100º 24' 07.77'' E	32 ± 1	57 ± 10	1,008.8 ± 0.6
BT	Diesel engine	05/08/07-07/08/07	6º 59' 42.78'' N	100º 28' 58.02'' E	33 ± 1	53 ± 3	1,008.1 ± 1.0
WI	Solid waste + Crude oil	08/08/07-10/08/08	6º 57' 15.43'' N	100º 24' 00.46'' E	31 ± 1	64 ± 8	1,007.8 ± 0.6
BF	Charcoal	15/08/07-17/08/07	7º 00' 23.09'' N	100º 30' 00.54'' E	32 ± 2	60 ± 2	1,007.8 ± 0.6
PR	Traffic	27/08/07-29/08/07	7º 00' 52.99'' N	100º 28' 20.50'' E	28 ± 3	73 ± 19	1,007.1 ± 2.0
KHH	Urban background	03/11/07-05/11/07	7º 00' 57.92'' N	100º 31' 12.76'' E	28 ± 2	73 ± 11	1,008.1 ± 0.0
RSB	Biomass burning	16/11/07	7º 27' 00.52'' N	100º 25' 19.02'' E	31	79	1,007.1
BB	Biomass burning	17/11/07	6º 57' 40.45'' N	100º 33' 06.68'' E	31	66	1,007.1
PTB	Biomass burning	18/11/07	6º 57' 40.45'' N	100º 33' 06.68'' E	27	79	1,006.1

[1]*T*, Temperature
[2]*RH*, Relative humidity
[3]*AP*, Air pressure

Table 2
Statistical summary of the concentration and fraction of organic carbon (OC), elemental carbon (EC) and OC/EC ratio.

Site	PM_{10} [μg m^{-3}]	TCA[a] [μg m^{-3}]	OC [μg m^{-3}]	EC [μg m^{-3}]	f_{OC}	f_{EC}	OC/EC
PSU1	35.7 ± 10.3	6.671 ± 8.391	4.838 ± 5.650	1.833 ± 0.856	0.136 ± 0.036	0.051 ± 0.006	2.640 ± 3.320
PSU2	27.9 ± 8.7	4.897 ± 3.640	3.573 ± 1.937	1.324 ± 0.673	0.128 ± 0.080	0.048 ± 0.028	2.699 ± 2.006
TI	46.9 ± 30.6	14.831 ± 37.439	8.572 ± 10.572	6.259 ± 13.786	0.183 ± 0.255	0.133 ± 0.306	1.370 ± 3.458
CI	35.9 ± 28.7	7.485 ± 15.925	5.230 ± 5.854	2.254 ± 4.079	0.146 ± 0.200	0.063 ± 0.124	2.320 ± 4.937
CPF	24.5 ± 5.4	7.385 ± 15.428	5.168 ± 4.448	2.217 ± 4.221	0.211 ± 0.187	0.090 ± 0.173	2.331 ± 4.869
SL1	13.8 ± 2.9	4.296 ± 2.000	3.063 ± 1.426	1.232 ± 0.268	0.222 ± 0.113	0.089 ± 0.019	2.486 ± 1.157
SL2	11.6 ± 3.7	0.977 ± 1.849	0.757 ± 0.397	0.221 ± 0.401	0.065 ± 0.040	0.019 ± 0.035	3.430 ± 6.489
RMF1	34.4 ± 8.6	15.829 ± 31.658	10.852 ± 17.158	4.977 ± 6.096	0.316 ± 0.505	0.145 ± 0.181	2.181 ± 4.361
RMF2	36.7 ± 15.7	11.022 ± 24.784	6.922 ± 10.449	4.100 ± 6.833	0.189 ± 0.296	0.112 ± 0.192	1.688 ± 3.796
BT	42.8 ± 24.9	14.112 ± 29.391	8.062 ± 8.154	6.050 ± 11.015	0.188 ± 0.219	0.141 ± 0.270	1.333 ± 2.775
WI	86.6 ± 65.4	24.449 ± 64.879	5.427 ± 11.266	19.023 ± 31.442	0.063 ± 0.139	0.220 ± 0.399	0.285 ± 0.757
BF	30.2 ± 14.1	6.280 ± 8.799	4.850 ± 2.611	1.430 ± 1.849	0.160 ± 0.114	0.047 ± 0.065	3.393 ± 4.754
PR	25.1 ± 9.2	9.650 ± 22.896	5.438 ± 8.693	4.212 ± 7.385	0.217 ± 0.356	0.168 ± 0.301	1.291 ± 3.063
KHH	9.6 ± 4.0	1.850 ± 1.224	1.352 ± 0.894	0.499 ± 0.055	0.141 ± 0.110	0.052 ± 0.022	2.711 ± 1.794
RSB	217.8 ± 96.1	80.362 ± 91.936	64.992 ± 51.974	15.370 ± 12.574	0.298 ± 0.273	0.071 ± 0.066	4.229 ± 4.838
BB	25.5 ± 2.3	11.106 ± 10.069	7.980 ± 2.234	3.126 ± 2.696	0.313 ± 0.092	0.123 ± 0.106	2.552 ± 2.314
PTB	83.7 ± 23.2	48.390 ± 66.486	38.578 ± 35.154	9.812 ± 10.090	0.461 ± 0.439	0.117 ± 0.125	3.932 ± 5.402

[a]Total carbonaceous aerosol (TCA) was calculated by the sum of organic matter.

DISCUSSION

To assess the health risks associated with the occupational exposure to PM_{10}, organic and elemental carbon of outdoor workers, the incremental lifetime particulate matter exposure (*ILPE*) model was employed and defined as:

$$ILPE = C \times IR \times t \times EF \times ED$$

Equation 5

where *ILPE* = incremental lifetime particulate matter exposure (g); *C* = PM_{10}, OC and EC concentrations (μg m^{-3}); *IR* = Inhalation rate (m^3 h^{-1}); *t* = Daily exposure time span (6 hours d^{-1}, for two shifts); *EF* = Exposure frequency (250 d $year^{-1}$ [a], upper-bound value); and *ED* = Exposure duration (25 years [a], upper-bound value) (Adapted from the Human Health Evaluation Manual, US EPA, 1991).

According to the methods for derivation of inhalation dosimetry (US EPA, 1994), the inhalation rates of male and female outdoor workers were estimated as 0.89 and 0.49 m^3 h^{-1}, respectively. The *ILPE* model was adapted from the probabilistic incremental lifetime cancer risk (*ILCR*) model, which was used to assess traffic policemen's exposure to PAHs at work in China (Hu *et al*, 2007). The estimated *ILPE* levels in outdoor workers are summarized in Table 3. The predicted *ILPE* of the carbonaceous species were consistently highest at RSB with average values of 2.682 ± 3.068 and 1.477 ± 1.689 g for TC accumulated in male and female workers, respectively, over a duration of 25 years. The data set was categorized into seven groups according to its source characteristics (Group 1: PSU1, PSU2, urban residential zone; Group 2: SL1, SL2, KHH, rural background; Group 3: TI, BT, PR, traffic emissions; Group 4: CPF, RMF1, RMF2, industrial activities; Group 5: RSB, BB, PTB, biomass burnings; Group 6: CI, WI, incinerator emissions; and Group 7: BF, charcoal burnings).

Using the results from Table 3, the individual percentage contributions of *ILPE* for each group to PM_{10}, TC, OC and EC were plotted and displayed in Fig 2. The main compositions of PM_{10} were Groups 5, 1, 6, 3, 7, 4 and 2, comprising 33.1, 32.1, 12.1, 7.56, 6.47, 6.19 and 2.46%, respectively. In comparison, a different distribution pattern of OC was observed, but the most abundant element was still Group 5, followed by Groups 6, 4, 3, 1, 7 and 2, constituting of 56.2, 15.5, 7.81, 7.77, 6.35, 4.66 and 1.74%, respectively. The characteristics of $ILPE_{max}$ observed in Group 5 for both PM_{10} and OC suggest the strong influence of biomass burning as an emission source of fine particulate matter and organic carbon in the atmosphere. This pattern of behavior supported the idea large scale forest fires emitted considerable amounts of fine aerosols and carbonaceous material into the atmosphere (Okuda *et al*, 2002).

Moreover, the results imply uncontrolled agricultural burning may play an important role in enhancing inhalation disease of the lungs in outdoor workers, such as farmers and/or residents who live adjacent to the rice fields. The major compositions of EC are Groups 6, 3, 5, 4, 1, 7 and 2, containing 39, 20.1, 12.3, 11.2, 7.94, 7.06 and 2.42%, respectively. The lowest percentage contribution ratio for Group 2 (*ie* rural background) supports the assumption the major source of EC is anthropogenic. Conversely, the highest EC content observed in Group 6 (*ie* corpse and waste incinerators) can be influenced by the "extremely high temperature" effect inside the ignition chamber as discussed previously. Whilst the second largest EC proportion which was detected in Group 3 (*ie* traffic sources) can be explained by imperfect combustions produced by diesel and petrol engines. Biomass burnings (*ie* Group 5) display negligible amounts of

EC emphasizing the adverse significance of forest fires on health. Incomplete combustion of heavy oil used in boilers of a fish processing factory (*ie* Group 4) also played an important role on EC concentrations in Hat Yai.

To obtain a quantitative understanding of the cancer risk, the gas-particle partitioning coefficients (K_P) of PAHs associated with different occupational environments were calculated according to Equation 1. As seen in Tables 4A and 4B, the highest K_P for all PAHs were in WI (-5.14 ~ 0.22), followed by PR (-5.40 ~ 0.02) and TI (-5.61 ~ -0.14). For the distribution of individual Log $K_{P\text{-}PAHs}$, an averaged Log $K_{P\text{-}D[a,h]A}$ was the highest (-0.61 ± 1.11), followed by Log $K_{P\text{-}B[g,h,i]P}$ (-0.63 ± 1.13) and Log $K_{P\text{-}Ind}$ (-0.75 ± 1.24), respectively. Because B[a]P is classified in Group II (*ie* probably carcinogenic to humans estimated on the basis of the feeding study of Neal and Rigdon (1967) using CFW strain mice), it is of great importance to conduct the sensitivity test relative to the highest Log $K_{P\text{-}B[a]P}$ of WI (Table 4B). The concept of normalization is introduced based on consideration of the Log $K_{P\text{-}B[a]P\text{-}other\ sites}$/ Log $K_{P\text{-}B[a]P\text{-}WI}$ ratio as illustrated in Fig 3. The average ratios of the Log $K_{P\text{-}B[a]P\text{-}other\ sites}$/ Log $K_{P\text{-}B[a]P\text{-}WI}$ for WI, PR and TI were 1.00, 0.77 and 0.64, respectively. These results strongly suggest regular exposure to PAHs in WI, PR and TI may be another leading cause of lung cancer, raising concerns regarding long term exposure in waste incinerator workers and policeman to fine particulate PAHs in Songkhla Province.

Recent work by Ribes *et al* (2003) demonstrated the ratio of $f_{SC}K_{SA}\delta_{OCT}/f_{OM}K_{OA}$ can be used as an indicator to determine the dominant gas-particle partitioning. This ratio will allow clarification of the prevalent mechanisms for gas-particle partitioning of PAHs. Dachs and Eisenreich (2000) suggested the mechanisms governing gas-particle partitioning of PAHs can be divided into three scenarios or cases according to the ratio of $f_{SC}K_{SA}\delta_{OCT}/f_{OM}K_{OA}$:

Case I: $\frac{f_{EC}K_{SA}\delta_{OCT}}{f_{OM}K_{OA}} > 5$

Case II: $5 > \frac{f_{EC}K_{SA}\delta_{OCT}}{f_{OM}K_{OA}} > 0.2$

Case III: $\frac{f_{EC}K_{SA}\delta_{OCT}}{f_{OM}K_{OA}} < 0.2$

Case I occurs when gas-particle partitioning is dominated by *ad*sorption onto the soot phase, Case III represents *ab*sorption into organic matter. Case II occurs when both *ab*sorption into the organic layer and *ad*sorption onto the soot carbon are the major sorptive mechanisms.

In this study, the ratios of $f_{SC}K_{SA}\delta_{OCT}/f_{OM}K_{OA}$ ranged from 21.73 to 0.31 with an average of 3.89 ± 4.71 for Ac, from 0.37 to 5.63 with an average of 1.00 ± 1.02 for B[a]P, from 1.05 to 15.95 with an average of 2.82 ± 3.47 for D[a,h]A and from 0.31 to 4.72 with an average of 0.83 ± 1.02 for Ind, respectively. Based on the ratios for $f_{SC}K_{SA}\delta_{OCT}/f_{OM}K_{OA}$, it seems reasonable to assume the major gas-particle partitioning of medium and high MW PAHs governing the atmosphere of urban residential zones, rural areas, industrial areas and biomass burning zones is *ab*sorption into the organic layer (Figs 4-6). Some studies reported that *ad*sorption and *de*sorption of semi-volatile organic compounds (SVOCs) to combustion aerosols may take hours to reach equilibrium and possibly due to the occurrence of a liquid-like organic film coating elemental carbon. Thus the mass transfer rate of SVOCs is limited by diffusion from the liquid-like organic phase into elemental carbon (Strommen and Kamens, 1999). Nevertheless, most PAHs in WI correspond to a $f_{SC}K_{SA}\delta_{OCT}/f_{OM}K_{OA}$ ratio higher

Table 3
Statistical description of the inhaled particulate mass of PM_{10}, total carbon (TC), organic carbon (OC) and elemental carbon (EC) at 15 sites in Songkhla Province, Thailand[a].

Site	PM_{10} [g][b] Male	PM_{10} [g][b] Female	TC [g][b] Male	TC [g][b] Female	OC [g][b] Male	OC [g][b] Female	EC [g][b] Male	EC [g][b] Female
PSU1	1.191 ± 0.344	0.656 ± 0.189	0.223 ± 0.280	0.123 ± 0.154	0.161 ± 0.189	0.089 ± 0.104	0.061 ± 0.029	0.034 ± 0.016
PSU2	0.930 ± 0.291	0.512 ± 0.160	0.163 ± 0.121	0.090 ± 0.067	0.119 ± 0.065	0.066 ± 0.036	0.044 ± 0.022	0.024 ± 0.012
TI	1.567 ± 1.021	0.863 ± 0.562	0.495 ± 1.250	0.273 ± 0.688	0.286 ± 0.353	0.158 ± 0.194	0.209 ± 0.460	0.115 ± 0.253
CI	1.199 ± 0.957	0.660 ± 0.527	0.250 ± 0.531	0.138 ± 0.293	0.175 ± 0.195	0.096 ± 0.108	0.075 ± 0.136	0.041 ± 0.075
CPF	0.818 ± 0.179	0.451 ± 0.099	0.246 ± 0.515	0.136 ± 0.283	0.172 ± 0.148	0.095 ± 0.082	0.074 ± 0.141	0.041 ± 0.078
SL1	0.461 ± 0.096	0.254 ± 0.053	0.143 ± 0.067	0.079 ± 0.037	0.102 ± 0.048	0.056 ± 0.026	0.041 ± 0.025	0.023 ± 0.005
SL2	0.388 ± 0.123	0.214 ± 0.068	0.033 ± 0.062	0.018 ± 0.034	0.025 ± 0.013	0.014 ± 0.007	0.007 ± 0.013	0.004 ± 0.007
RMF1	1.147 ± 0.287	0.632 ± 0.158	0.528 ± 1.057	0.291 ± 0.582	0.362 ± 0.573	0.199 ± 0.315	0.166 ± 0.203	0.091 ± 0.112
RMF2	1.224 ± 0.525	0.674 ± 0.289	0.368 ± 0.827	0.203 ± 0.455	0.231 ± 0.349	0.127 ± 0.192	0.137 ± 0.228	0.075 ± 0.126
BT	1.430 ± 0.830	0.787 ± 0.457	0.471 ± 0.981	0.259 ± 0.540	0.269 ± 0.272	0.148 ± 0.150	0.202 ± 0.368	0.111 ± 0.202
WI	2.889 ± 2.184	1.590 ± 1.203	0.816 ± 2.165	0.449 ± 1.192	0.181 ± 0.376	0.100 ± 0.207	0.635 ± 1.049	0.350 ± 0.578
BF	1.009 ± 0.470	0.556 ± 0.259	0.210 ± 0.294	0.115 ± 0.162	0.162 ± 0.087	0.089 ± 0.048	0.048 ± 0.062	0.026 ± 0.034
PR	0.837 ± 0.307	0.461 ± 0.169	0.322 ± 0.764	0.177 ± 0.421	0.182 ± 0.290	0.100 ± 0.160	0.141 ± 0.246	0.077 ± 0.136
KHH	0.319 ± 0.132	0.176 ± 0.073	0.062 ± 0.041	0.034 ± 0.022	0.045 ± 0.030	0.025 ± 0.016	0.017 ± 0.002	0.009 ± 0.001
RSB	7.267 ± 3.207	4.001 ± 1.766	2.682 ± 3.068	1.477 ± 1.689	2.169 ± 1.735	1.194 ± 0.955	0.513 ± 0.420	0.282 ± 0.231
BB	0.851 ± 0.076	0.469 ± 0.042	0.371 ± 0.336	0.204 ± 0.185	0.266 ± 0.075	0.147 ± 0.041	0.104 ± 0.090	0.057 ± 0.050
PTB	2.792 ± 0.776	1.537 ± 0.427	1.615 ± 2.219	0.889 ± 1.222	1.288 ± 1.173	0.709 ± 0.646	0.327 ± 0.337	0.180 ± 0.185

[a]Inhaled particulate mass over exposure duration of 25 years.
[b]Values represent average ± standard deviation.

Table 4A
Statistical description of the estimated Log K_p of PAHs at 15 sites in Songkhla Province, Thailand[a].

	Log K_P Ac	Log K_P Ace	Log K_P Fl	Log K_P Ph	Log K_P An	Log K_P Fluo	Log K_P Pyr
PSU1	-6.95 ± 7.52	-6.80 ± 7.37	-6.46 ± 7.02	-5.78 ± 6.30	-5.75 ± 6.26	-4.83 ± 5.30	-4.78 ± 5.27
PSU2	-6.01 ± 6.86	-5.86 ± 6.71	-5.52 ± 6.36	-4.83 ± 5.66	-4.79 ± 5.62	-3.86 ± 4.67	-3.82 ± 4.64
TI	-5.61 ± 5.95	-5.46 ± 5.80	-5.12 ± 5.45	-4.41 ± 4.73	-4.38 ± 4.70	-3.44 ± 3.74	-3.40 ± 3.71
CI	-5.91 ± 6.29	-5.76 ± 6.15	-5.42 ± 5.81	-4.74 ± 5.13	-4.71 ± 5.09	-3.79 ± 4.17	-3.74 ± 4.13
CPF	-5.90 ± 6.44	-5.76 ± 6.31	-5.43 ± 5.97	-4.75 ± 5.29	-4.72 ± 5.26	-3.81 ± 4.35	-3.76 ± 4.30
SL1	-5.86 ± 6.85	-5.72 ± 6.71	-5.38 ± 6.38	-4.69 ± 5.71	-4.65 ± 5.68	-3.73 ± 4.78	-3.68 ± 4.73
SL2	-6.59 ± 6.98	-6.45 ± 6.84	-6.11 ± 6.50	-5.43 ± 5.82	-5.40 ± 5.79	-4.48 ± 4.88	-4.44 ± 4.83
RMF1	-5.88 ± 6.47	-5.73 ± 6.33	-5.39 ± 5.99	-4.71 ± 5.31	-4.68 ± 5.28	-3.76 ± 4.36	-3.72 ± 4.31
RMF2	-5.93 ± 6.76	-5.79 ± 6.62	-5.46 ± 6.29	-4.78 ± 5.62	-4.75 ± 5.59	-3.84 ± 4.69	-3.79 ± 4.64
BT	-5.72 ± 6.19	-5.58 ± 6.04	-5.24 ± 5.70	-4.57 ± 5.01	-4.53 ± 4.97	-3.62 ± 4.04	-3.57 ± 4.00
WI	-5.14 ± 5.00	-5.00 ± 4.86	-4.66 ± 4.52	-3.98 ± 3.83	-3.95 ± 3.80	-3.02 ± 2.88	-2.98 ± 2.83
BF	-6.08 ± 6.65	-5.94 ± 6.52	-5.60 ± 6.19	-4.92 ± 5.53	-4.89 ± 5.50	-3.98 ± 4.61	-3.93 ± 4.55
PR	-5.40 ± 5.53	-5.26 ± 5.38	-4.91 ± 5.05	-4.22 ± 4.36	-4.18 ± 4.33	-3.25 ± 3.41	-3.21 ± 3.36
KHH	-6.10 ± 6.62	-5.96 ± 6.47	-5.61 ± 6.11	-4.92 ± 5.40	-4.88 ± 5.37	-3.95 ± 4.41	-3.91 ± 4.38
RSB	-6.74 ± 7.00	-6.60 ± 6.85	-6.26 ± 6.51	-5.57 ± 5.83	-5.53 ± 5.79	-4.60 ± 4.86	-4.56 ± 4.82
BB	-5.90 ± 6.77	-5.76 ± 6.63	-5.42 ± 6.29	-4.73 ± 5.60	-4.69 ± 5.56	-3.77 ± 4.63	-3.72 ± 4.59
PTB	-6.11 ± 6.54	-5.97 ± 6.40	-5.62 ± 6.05	-4.92 ± 5.35	-4.89 ± 5.32	-3.95 ± 4.38	-3.91 ± 4.34

[a]Values represent average ± standard deviation.

Table 4B
Statistical description of the estimated Log K_p of PAHs at 15 sites in Songkhla Province, Thailand[a].

	Log K_P B[*a*]A	Log K_P Chry	Log K_P B[*a*]P	Log K_P Ind	Log K_P D[*a*,*h*]A	Log K_P B[*g*,*h*,*i*]P
PSU1	-3.78 ± 4.27	-3.46 ± 3.89	-2.49 ± 2.92	-1.72 ± 2.13	-1.58 ± 1.98	-1.61 ± 2.01
PSU2	-2.82 ± 3.63	-2.48 ± 3.27	-1.51 ± 2.30	-0.73 ± 1.51	-0.59 ± 1.37	-0.62 ± 1.40
TI	-2.40 ± 2.70	-2.04 ± 2.31	-1.07 ± 1.34	-0.28 ± 0.55	-0.14 ± 0.40	-0.16 ± 0.43
CI	-2.74 ± 3.12	-2.43 ± 2.80	-1.45 ± 1.83	-0.68 ± 1.06	-0.55 ± 0.92	-0.57 ± 0.95
CPF	-2.76 ± 3.30	-2.45 ± 3.00	-1.48 ± 2.02	-0.72 ± 1.26	-0.58 ± 1.12	-0.61 ± 1.15
SL1	-2.68 ± 3.73	-2.35 ± 3.45	-1.38 ± 2.48	-0.60 ± 1.72	-0.47 ± 1.59	-0.49 ± 1.61
SL2	-3.44 ± 3.83	-3.12 ± 3.52	-2.15 ± 2.55	-1.38 ± 1.78	-1.25 ± 1.64	-1.27 ± 1.67
RMF1	-2.71 ± 3.31	-2.40 ± 2.99	-1.42 ± 2.02	-0.65 ± 1.24	-0.52 ± 1.11	-0.54 ± 1.13
RMF2	-2.79 ± 3.64	-2.49 ± 3.35	-1.52 ± 2.38	-0.76 ± 1.63	-0.62 ± 1.49	-0.65 ± 1.52
BT	-2.58 ± 3.00	-2.27 ± 2.66	-1.30 ± 1.69	-0.53 ± 0.91	-0.40 ± 0.78	-0.42 ± 0.80
WI	-1.98 ± 1.83	-1.66 ± 1.51	-0.69 ± 0.54	0.09 ± 0.23	0.22 ± 0.37	0.20 ± 0.35
BF	-2.93 ± 3.56	-2.62 ± 3.29	-1.65 ± 2.31	-0.89 ± 1.56	-0.75 ± 1.43	-0.78 ± 1.46
PR	-2.21 ± 2.36	-1.87 ± 2.03	-0.90 ± 1.07	-0.12 ± 0.30	0.02 ± 0.16	-0.003 ± 0.18
KHH	-2.90 ± 3.37	-2.56 ± 3.00	-1.59 ± 2.03	-0.81 ± 1.24	-0.67 ± 1.10	-0.69 ± 1.12
RSB	-3.55 ± 3.82	-3.23 ± 3.49	-2.25 ± 2.51	-1.47 ± 1.74	-1.34 ± 1.60	-1.36 ± 1.63
BB	-2.72 ± 3.59	-2.39 ± 3.26	-1.42 ± 2.29	-0.64 ± 1.51	-0.51 ± 1.37	-0.53 ± 1.40
PTB	-2.90 ± 3.33	-2.55 ± 2.98	-1.58 ± 2.01	-0.80 ± 1.23	-0.66 ± 1.09	-0.69 ± 1.12

[a]Values represent average ± standard deviation.

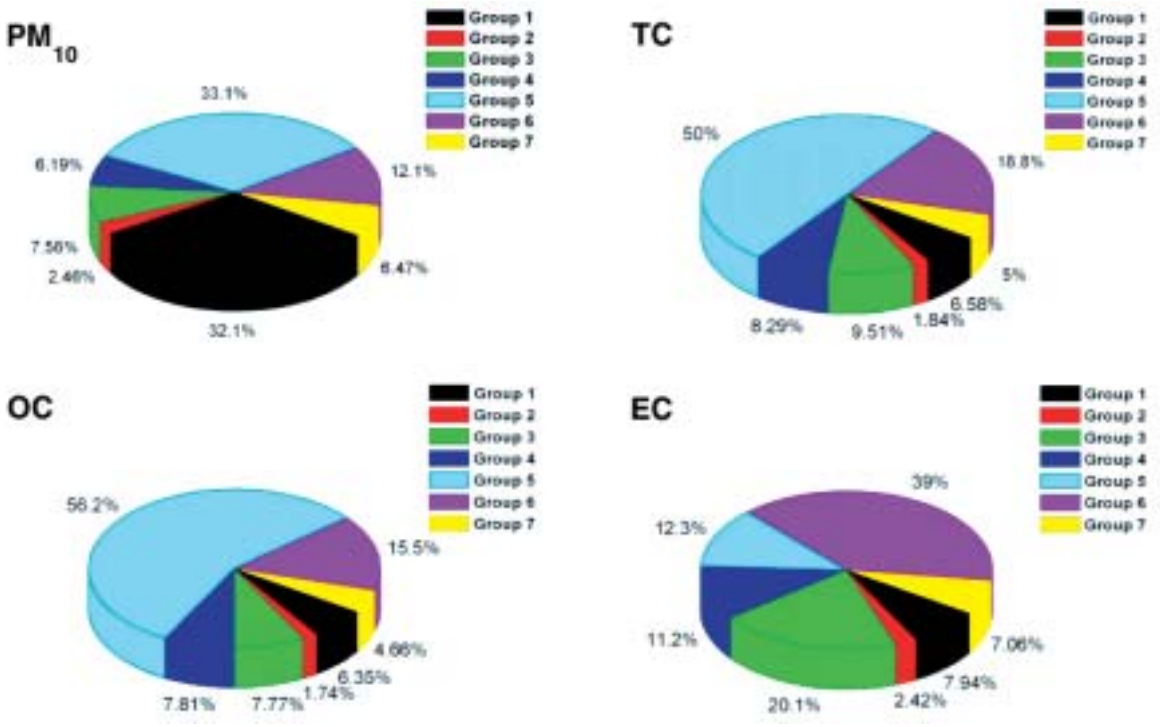

Fig 2– Averaged percentage contributions of Group 1: PSU1,PSU2, urban residential zone; Group 2: SL1, SL2, KHH, rural background; Group 3: TI, BT, PR, traffic emissions; Group 4: CPF, RMF1, RMF2, industrial activities; Group 5: RSB, BB, PTB, biomass burnings; Group 6: CI, WI, incinerator emissions; Group 7: BF, charcoal burnings in PM10, TC, OC and EC.

than 5 (Case I) and thus one can conclude that *ad*sorption entirely dominated gas-particle partitioning of PAHs in a waste incinerator (Figs 4-6). *Ab*sorption into organic matter accounted for less than 10% of the total PAHs in Chesapeake Bay particulate phase (Dachs *et al*, 2000). Interestingly, both *ab*sorption into the organic layer and *ad*sorption on the soot phase played a major role in gas-particle partitioning of low MW PAHs observed at heavy traffic area (*ie* TI, BT, PR) and in a rubber manufacturing zone (RMF1, RMF2).

Despite the various efforts described above to explain the dominant gas-particle partitioning, it is difficult to provide a completely clear picture of the relative importance of OC and EC in the gas-particle partitioning of the PAHs of interest here. For instance, the confounding effects of another sorptive compartment, such as mineral surfaces, may exist. The uncertainties in OC and EC determinations and measurement artifacts rule out the role for *ad*sorption onto particle surfaces. Finally, the assistance of some correlation between the *ab*sorptive properties of the OC with the amount of EC and/or some correlation between the *ad*-sorptive properties of the EC with the amount of OC causes errors in model evaluation. Therefore, multiple methods and aspects are crucial to explain three contrasting descriptions (*ie ab*sorption, *ad*sorption and *ab/ad*-sorption) of the gas-particle partitioning of PAHs.

In summary, This study found a substantial risk for lung cancer in workers in

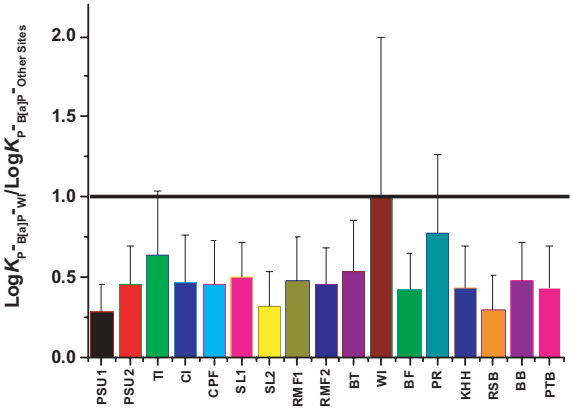

Fig 3–The average ratios of Log $K_{P\text{-}B[a]P\text{-}other\ sites}$/ Log $K_{P\text{-}B[a]P\text{-}WI}$.

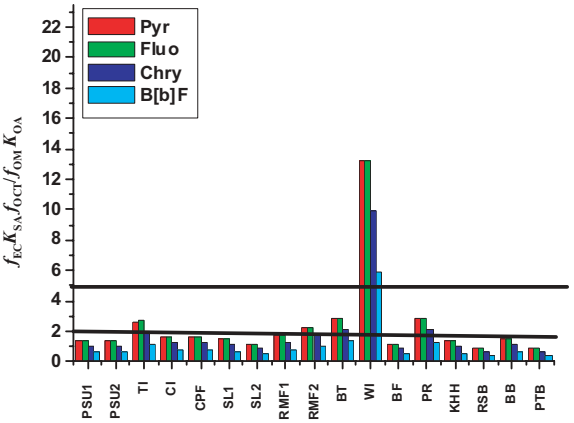

Fig 5–The ratios of $f_{EC}K_{SA}f_{OCT}/f_{OM}K_{OA}$ of Pyr, Fluo, Chry and B[b]F.

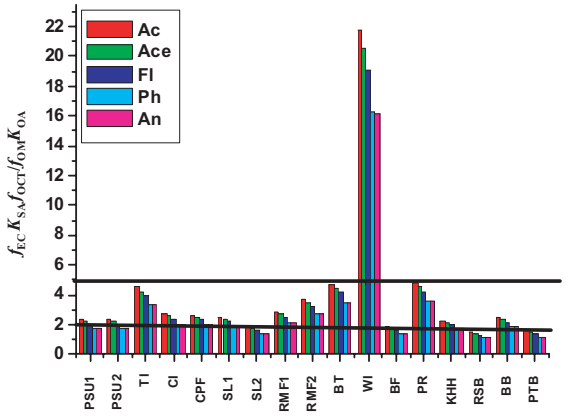

Fig 4–The ratios of $f_{EC}K_{SA}f_{OCT}/f_{OM}K_{OA}$ of Ac, Ace, Fl, Ph and An.

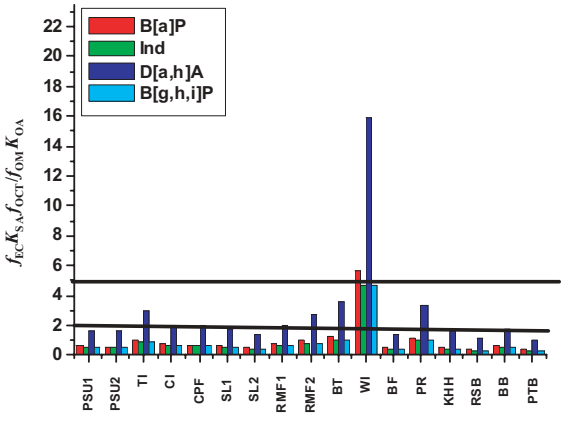

Fig 6–The ratios of $f_{EC}K_{SA}f_{OCT}/f_{OM}K_{OA}$ of B[a]P, Ind, D[a,h]A and B[g,h,i]P.

waste incinerator plants, traffic intersections and bus terminals. The characteristics of $ILPE_{max}$ observed with the biomass burning group in both PM_{10} and OC supported the idea large scale forest fires may be responsible for the large amounts of fine carbonaceous aerosols injected into the atmosphere and thus raising concerns of significant deterioration of air quality during the EL Nino period. The analysis of $f_{SC}K_{SA}\delta_{OCT}/f_{OM}K_{OA}$ ratios indicates the overwhelming mechanisms of *ad*sorption in gas-particle partitioning for all PAHs in the waste incinerator, and *ab*sorption tends to dominate the gas-particle partitioning of medium and high MW PAHs in urban residential zones, rural areas and other emission sources. Interestingly, the dual mode of *ab*/*ad*sorption plays a major role in gas-particle partitioning of low MW PAHs in traffic emission sources.

ACKNOWKEDGEMENTS

The authors would like to thank the Synchrotron Light Research Institute (Public Organization), Ministry of Science and Technology, Royal Thai Government and the National Center of Excellence for Environmental and Hazardous Waste Management-PSU Satellite Center, Prince of Songkla University, for continued financial support of this work.

REFERENCES

Dachs J, Eisenreich SJ. *Ad*sorption onto aerosol soot carbon dominates gas-particle partitioning of polycyclic aromatic hydrocarbons. *Environ Sci Technol* 2000; 34: 3690-7.

Fenizio A, Mackay D, Bidleman T, Harners T. Octanol-air partition coefficient as a predictor of partitioning of semi-volatile organic chemicals to aerosols. *Atmos Environ* 1997; 31: 2289-96.

Fernandez P, Grimalt JO, Vilanova RM. Atmospheric gas-particle partitioning of polycyclic aromatic hydrocarbons in high mountain regions of Europe. *Environ Sci Technol* 2002; 36: 1162-8.

Harner T, Bidleman TF. Octanol–air partition coefficient for describing particle/gas partitioning of aromatic compounds in urban air. *Environ Sci Technol* 1998a; 32: 1494-502.

Harner T, Bidleman TF. Measurement of octanol–air partition coefficients for polycyclic aromatic hydrocarbons and polychlorinated naphthalenes. *J Chem Eng Data* 1998b; 43: 40-6.

Harvey RG. Polycyclic aromatic hydrocarbons. Cambridge, USA: Cambridge University Press, 1991.

Hu Y, Bai Z, Zhang L, Wang X, Zhang LY, Qingchan ZT. Health risk assessment for traffic policemen exposed to polycyclic aromatic hydrocarbons (PAHs) in Tianjin, China. *Sci Total Environ* 2007; 382: 240-50.

IARC. Overall evaluations of carcinogenicity: An updating of IARC monographs. Monographs on the evaluation of carcinogenic risks to humans. Lyon: International Agency for Research on Cancer, 1987; 1-42 (suppl 7).

IARC. Polychlorinated dibenzo-para-dioxins and polychlorinated dibenzofurans, monographs on the evaluation of carcinogenic risks to humans. Lyon: International Agency for Research on Cancer, 1997; 69.

Jonker MTO, Koelmans AA. Sorption of polycyclic aromatic hydrocarbons and polychlorinated biphenyls to soot and soot-like materials in the aqueous environment: mechanistic considerations. *Environ Sci Technol* 2002; 36: 3725-34.

Korenaga T, Liu XX, Huang ZY. The influence of moisture content on polycyclic aromatic hydrocarbons emission during rice straw burning. Chemosphere – Global Change. *Science* 2001; 3: 117-22.

Mastral AM, Callén M S. A review on polycyclic aromatic hydrocarbon (PAH) emissions from energy generation. *Environ Sci Technol* 2000; 34: 3051-7.

Menzie CA, Potocki BB, Santodonato J. Exposure to carcinogenic PAHs in the environment. *Environ Sci Technol* 1992; 26: 1278-84.

Na K, Cocker III DR. Organic and elemental carbon concentrations in fine particulate matter in residence, schoolrooms, and outdoor air in Mira Loma, California. *Atmos Environ* 2005; 39: 3325-33.

Neal J, Rigdon RH. Gastric tumors in mice fed benzo[a]pyrene: a quantitative study. *Tex Rep Biol* Med 1967; 25: 553.

Odabasi M, Cetin E, Sofuoglu A. Determination of octanol–air partition coefficients and supercooled liquid vapor pressures of PAHs as a function of temperature: Application to gas–particle partitioning in an urban atmosphere. *Atmos Environ* 2006; 40: 6615-25.

Ohura T, Amagai T, Fusaya M, Matsushita H. Spatial distributions and profiles of atmospheric polycyclic aromatic hydrocarbons in two industrial cities in Japan. *Environ Sci Technol* 2004; 38: 49-55.

Okuda T, Kumata H, Zakaria MP, Naraoka H, Ishiwatari R, Takada H. Source identifica-

tion of Malaysian atmospheric polycyclic aromatic hydrocarbons nearby forest fires using molecular and isotopic compositions. *Atmos Environ* 2002; 36: 611-8.

Pankow JF. An *ab*sorption model of gas/particle partitioning of organic compounds in the atmosphere. *Atmos Environ* 1994a; 28: 185-8.

Pankow JF. An *ab*sorption model of the gas/aerosol partitioning involved in the formation of secondary organic aerosol. *Atmos Environ* 1994b; 28: 189-93.

Pankow JF. A consideration of the role of gas/particulate partitioning in the deposition of nicotine and other tobacco smoke compounds in the respiratory track. *Chem Res Toxicol* 2001; 14: 1465-81.

Repace J. Respirable particles and carcinogens in the air of Delaware hospitality venues before and after a smoking ban. *J Occup Environ Med* 2004; 46: 887-905.

Ribes S, Drooge BV, Dachs J, Gustafsson ÿ, Grimalt JO. Influence of soot carbon on the soil-air partitioning of polycyclic aromatic hydrocarbons. *Environ Sci Technol* 2003; 37: 2675-80.

Sanderson EG, Farant JP. Use of benzo[*a*]pyrene relative abundance ratios to assess exposure to polycyclic aromatic hydrocarbons in the ambient atmosphere in the vicinity of a Söderberg aluminum smelter. *J Air Waste MA* 2000; 50: 2085-92.

Simcik MF, Franz TP, Zhang HX, Eisenreich SJ. Gas–particle partitioning of PCBs and PAHs in the Chicago urban and adjacent coastal atmosphere: states of equilibrium. *Environ Sci Technol* 1998; 32: 251-7.

Sitaras IE, Bakeas EB, Siskos PA. Gas/particle partitioning of seven polycyclic aromatic hydrocarbons in a heavy traffic urban area. *Sci Total Environ* 2004; 327: 249-64.

Strommen MR, Kamens RM. Simulation of semivolatile organic compound microtransport at different time scales in airborne diesel soot particles. *Environ Sci Technol* 1999; 33: 1738-46.

Tasdemir Y, Esen F. Urban air PAHs: Concentrations, temporal changes and gas/particle partitioning at a traffic site in Turkey. *Atmos Res* 2007; 84: 1-12.

Turpin BJ, Lim HJ. Species contributions to $PM_{2.5}$ mass concentrations: revisiting common assumptions for estimating organic mass. *Aerosol Sci Technol* 2001; 35: 602-10.

US EPA. Risk assessment guidance for superfund. Vol 1. Human health evaluation manual, supplemental guidance: "Standard default exposure factors" interim final. Washington D.C. OSWER Directive 9285.6-03, 1991.

US EPA. Methods for derivation of inhalation dosimetry. Washington DC: Office of Research and Development, Office of Health and Environmental Assessment. EPA/600/Z-92/001. 1994

Vardar N, Tasdemir Y, Odabasi M, Noll KE. Characterization of atmospheric concentrations and partitioning of PAHs in the Chicago atmosphere. *Sci Total Environ* 2004; 327: 163-74.

Wold Health Organization (WHO). Air quality guidelines for Europe. 2nd ed. *WHO Eur Ser* 2000; 91.